Localization of Brain Electrical Activity via Linearly Constrained Minimum Variance Spatial Filtering

Barry D. Van Veen,* *Member, IEEE,* Wim van Drongelen, Moshe Yuchtman, and Akifumi Suzuki

***Abstract*— A spatial filtering method for localizing sources of brain electrical activity from surface recordings is described and analyzed. The spatial filters are implemented as a weighted sum of the data recorded at different sites. The weights are chosen to minimize the filter output power subject to a linear constraint. The linear constraint forces the filter to pass brain electrical activity from a specified location, while the power minimization attenuates activity originating at other locations. The estimated output power as a function of location is normalized by the estimated noise power as a function of location to obtain a neural activity index map. Locations of source activity correspond to maxima in the neural activity index map. The method does not require any prior assumptions about the number of active sources of their geometry because it exploits the spatial covariance of the source electrical activity. This paper presents a development and analysis of the method and explores its sensitivity to deviations between actual and assumed data models. The effect on the algorithm of covariance matrix estimation, correlation between sources, and choice of reference is discussed. Simulated and measured data is used to illustrate the efficacy of the approach.**

***Index Terms*— Dipole localization, EEG localization, linearly constrained minimum variance filter, MEG localization, reference electrode, spatial filtering.**

I. Introduction

In current clinical practice, neural activity in the brain is often recorded from scalp electrodes. The ongoing electroencephalogram and the potentials evoked by stimulation reflect activity from groups of neurons located in the head. Finding the sources responsible for generating this activity is a central issue in neurophysiology. Knowledge of the anatomical correlate of recorded activity is essential for diagnosis and treatment. Currently, more detailed anatomical information about abnormally active areas is obtained by implanting depth electrodes in several locations. Clinically and experimentally, one would like to avoid recording inside neural tissue, because the technique is invasive, delicate, and time consuming. Moreover, one cannot have depth electrodes at all potentially active sites, so one can overlook areas of interest.

These reasons have motivated many studies that attempt to formalize a relationship between electromagnetic activity in the head and external recordings of the generated field [1]–[15]. These models represent underlying neural activity by either a charge or current dipole. Starting from a known activity pattern in the brain, one can calculate the electromagnetic field generated outside the brain in a unique fashion. This so-called forward solution depends on a number of parameters related to the geometry of the anatomical model and the electromagnetic properties of the different tissues. Some studies use a spherical model describing the head [1], [2], [5]–[8], while others refine the geometric representation by using finite element or boundary element methods [3], [4], [9], [13]. The experimental and clinical problem, however, is the inverse problem: the field is sampled at different sensor locations and the underlying activity pattern must be determined. A given set of measurements cannot generate a unique solution for the activities inside the head. To obtain a single inverse solution for a given recording, additional constraints are introduced. A problem common to all methods is determining the number of active areas that contribute to the signal studied. Some authors assume a single generator at every time instant (see e.g., [1]); others use a linear decomposition of a recorded interval as a tool to estimate the number of active sites (see e.g., [8]).

In this paper, we develop a localization method based on the principles of spatial filtering. Spatial filters are designed that pass brain electrical activity from a specified location while attenuating activity originating at other locations. The power at the output of a spatial filter is an estimate of the neural power originating within the spatial passband of the filter. A map of neural power as a function of location is obtained by designing multiple spatial filters, each with a different passband, and depicting output power as a function of passband location. This spatial filtering approach represents an adaptation of the multiple window minimum variance spectrum estimation method proposed by Liu and Van Veen [16] and falls within the general category of linearly constrained minimum variance (LCMV) filtering. Spatial filtering or "beamforming" using LCMV methods has been widely applied in radar and sonar [17]. Early work on LCMV beamforming includes [18] and [19].

The map of neural power would appear to provide a useful metric for source localization by associating sources with regions of large neural power. However, we show that noise introduces a spatially non uniform component to the neural power map that depends on the measurement sites. Hence, noise may cause false detection of sources or missed detection of actual sources in the neural power map. This problem is

Manuscript received January 17, 1996; revised May 1, 1997. *Asterisk indicates corresponding author.*

*B. D. Van Veen is with the Department of Electrical and Computer Engineering, University of Wisconsin, 1415 Engineering Drive, Madison, WI 53706 USA (e-mail: vanveen@engr.wisc.edu).

W. van Drongelen and M. Yuchtman are with Nicolet Biomedical, Inc., Madison, WI 53744-4451 USA.

A. Suzuki is with the Department of Surgical Neurology, Research Institute for Brain and Bloodvessels, Akita 010 Japan.

Publisher Item Identifier S 0018-9294(97)06114-4.

mitigated by normalizing the neural power map by an estimate of the noise power map to obtain a neural activity index. Localization is accomplished by identifying local maxima in the neural activity index as sources.

The present approach does not require any prior assumptions about the number or spatial distribution of active sources. Indeed, under the appropriate conditions both the number and locations of sources can be determined. Distributed sources such as dipole sheets can also be identified given adequate signal-to-noise ratio (SNR). Prior source information is not required because the localization is performed using the spatial covariance matrix of the surface data. Guidelines for estimating the spatial covariance matrix from measured data are discussed.

Theoretical considerations in applying the LCMV method to neurophysiology were previously reported in [11] and [20]. Related ideas have also been reported in the literature. An application of spatial filtering to monitoring specific regions of the brain has been discussed by Spencer *et al.* [21]. Dale and Sereno [12] require estimates of dipole variance needed in their constrained linear approach to solving the inverse problem. The method used to estimate the dipole variance is based on the MUSIC algorithm [10] and is similar in certain aspects to the approach taken here. Description of the similarities and differences is provided in the discussion section. van Drongelen *et al.* [22] use the LCMV localization technique with simulated and measured electrophysiological data in order to explore the method's resolving power and ability to detect multiple sources. In the present paper, we provide a detailed exposition of the LCMV method and study the sensitivity of the approach to deviation between the actual and assumed data models.

II. Data Model

The LCMV approach is based on source and head models that relate the underlying neural activity to the distribution of potential (electric, magnetic, or both) measured at the surface. This section develops these models and relates them to the first- and second-order statistics of the data. For notation, lower- and upper-case boldface symbols represent vector and matrix quantities, respectively. Superscript T denotes matrix transpose and superscript -1 matrix inverse. The trace of the matrix $\mathbf{A}$ is written as $\mathrm{tr}\{\mathbf{A}\}$.

The current dipole is a key component of our model relating the surface measurements to the underlying neural activity. An individual active neuron is reasonably modeled as a current dipole. Active areas in the cortex can be modeled by an equivalent electrical dipole. The relationship between dipole models and the surface recordings is obtained as follows.

Let $\mathbf{x}$ be an $N \times 1$ vector composed of the potentials measured at the N electrode sites at a given instant in time associated with a single dipole source. If this source has location represented by the 3×1 vector $\mathbf{q}$, then $\mathbf{x} = \mathbf{H}(\mathbf{q})\mathbf{m}(\mathbf{q})$ where the elements of the 3×1 vector $\mathbf{m}(\mathbf{q})$ are the x, y, and z components of the dipole moment at the instant in time $\mathbf{x}$ is measured and the columns of the $N \times 3$ transfer matrix $\mathbf{H}(\mathbf{q})$ represent solutions to the forward problem. That is, the first column of $\mathbf{H}(\mathbf{q})$ is the potential at the electrodes due to a dipole source at location $\mathbf{q}$ having unity moment in the x direction and zero moment in y and z directions. Similarly, the second and third columns represent the potential due to sources with unity moment in y and z directions, respectively. Note that this model for the data applies to electric, magnetic, or combined electric and magnetic measurements. Only the elements of $\mathbf{H}(\mathbf{q})$ depend on the particular sensing modality. In a physical sense, $\mathbf{H}(\mathbf{q})$ represents the material and geometrical properties of the medium in which the sources are submerged.

The medium is linear so the potential at the scalp is the superposition of the potentials from many active neurons. Suppose $\mathbf{x}$ is composed of the potentials due to L active dipole sources at locations $\mathbf{q}_i$, $i = 1, 2, \cdots, L$ and noise. Then

$$\mathbf{x} = \sum_{i=1}^{L} \mathbf{H}(\mathbf{q}_i)\mathbf{m}(\mathbf{q}_i) + \mathbf{n} \tag{1}$$

where $\mathbf{m}(\mathbf{q}_i)$ is the dipole moment at location $\mathbf{q}_i$ and $\mathbf{n}$ is the measurement noise. For very large L the sum may be represented as an integral over the volume containing possible sources. Note that $\mathbf{x}$ does not contain any temporal information since it is obtained by sampling all electrodes at a single time instant. It represents the spatial distribution of potential at the measurement sites at the sampling time.

The electrical activity of an individual neuron is assumed to be a random process influenced by external inputs to the neuron. Hence, we model the dipole moment as a random quantity and describe its behavior in terms of mean and covariance. Specifically, we denote the moment mean vector $\overline{\mathbf{m}}(\mathbf{q}_i)$, and covariance matrix $\mathbf{C}(\mathbf{q}_i)$ as

$$\overline{\mathbf{m}}(\mathbf{q}_i) = E\{\mathbf{m}(\mathbf{q}_i)\} \tag{2}$$

$$\mathbf{C}(\mathbf{q}_i) = E\{[\mathbf{m}(\mathbf{q}_i) - \overline{\mathbf{m}}(\mathbf{q}_i)]\,[\mathbf{m}(\mathbf{q}_i) - \overline{\mathbf{m}}(\mathbf{q}_i)]^T\}. \tag{3}$$

Assuming the noise is zero mean ($E\{\mathbf{n}\} = \mathbf{0}$) with covariance matrix $\mathbf{Q}$ and that the moments associated with different dipoles are uncorrelated, that is

$$E\{[\mathbf{m}(\mathbf{q}_i) - \overline{\mathbf{m}}(\mathbf{q}_i)]\,[\mathbf{m}(\mathbf{q}_k) - \overline{\mathbf{m}}(\mathbf{q}_k)]^T\} = \mathbf{0} \tag{4}$$

then

$$\begin{aligned}\overline{\mathbf{m}}(\mathbf{x}) &= E\{\mathbf{x}\} \\ &= \sum_{i=1}^{L} \mathbf{H}(\mathbf{q}_i)\overline{\mathbf{m}}(\mathbf{q}_i)\end{aligned} \tag{5}$$

$$\begin{aligned}\mathbf{C}(\mathbf{x}) &= E\{[\mathbf{x} - \overline{\mathbf{m}}(\mathbf{x})]\,[\mathbf{x} - \overline{\mathbf{m}}(\mathbf{x})]^T\} \\ &= \sum_{i=1}^{L} \mathbf{H}(\mathbf{q}_i)\mathbf{C}(\mathbf{q}_i)\mathbf{H}^T(\mathbf{q}_i) + \mathbf{Q}\end{aligned} \tag{6}$$

represent the mean and the covariance matrix of the observed data vector $\mathbf{x}$, respectively.

The variance associated with a particular source is a measure of the strength of the source and is defined as the sum of the variance of each component of the dipole moment or

$$\mathrm{Var}\,(\mathbf{q}) = \mathrm{tr}\,\{\mathbf{C}(\mathbf{q})\}. \tag{7}$$

We estimate this variance by determining how much of the covariance matrix is consistent with the transfer matrix for a given location.

Electrical data is collected as a potential measured with respect to a reference electrode. Our experience indicates that the LCMV method is generally insensitive to the choice of reference electrode. This observation is based on obtaining virtually identical results when using the same data set but recomputing the potentials with respect to differing electrodes (see, e.g., Section V-B). However, it is straightforward to preprocess the data to guarantee that all results are independent of the reference electrode.

The effect of the reference is to add a constant, unknown potential to each electrode. This is expressed mathematically as follows. If $\mathbf{x}_1$ and $\mathbf{x}_2$ are potentials measured at the same set of electrodes with respect to different reference electrodes, then

$$\mathbf{x}_2 = \mathbf{x}_1 + c\mathbf{1} \tag{8}$$

where $\mathbf{1}$ is a vector of all ones and c is the unknown difference in potential between the two reference electrodes. The effect of the reference is eliminated if we apply a transformation to the data that is orthogonal to the $\mathbf{1}$ vector. Define an N by $N-1$ matrix $\mathbf{T}$ satisfying

$$\begin{aligned} \mathbf{T}^T\mathbf{1} &= \mathbf{0} \\ \text{rank}\,\{\mathbf{T}\} &= N-1. \end{aligned} \tag{9}$$

That is, the $N-1$ linearly independent columns of $\mathbf{T}$ all sum to zero. Such a $\mathbf{T}$ is easily constructed using a matrix orthogonalization procedure, such as the QR decomposition. Note that (9) implies $\mathbf{T}^T\mathbf{x}_2 = \mathbf{T}^T\mathbf{x}_1$. Hence, reference free data is obtained as

$$\mathbf{x}^f = \mathbf{T}^T\mathbf{x}. \tag{10}$$

Substitution of (1) into (10) indicates that the transfer matrices $\mathbf{H}(\mathbf{q})$ must also be modified by the transformation $\mathbf{T}$. Specifically, $\mathbf{H}^f(\mathbf{q}) = \mathbf{T}^T\mathbf{H}(\mathbf{q})$. A second consequence of removing the reference is the loss of one degree of freedom, as manifest in the reduction from N dimensional data vectors $\mathbf{x}$ to $N-1$ dimensional data vectors $\mathbf{x}^f$. This loss is a result of ignoring all components of the data that lie in the one dimensional space spanned by $\mathbf{1}$. Components in this space are of marginal utility anyway, since one can never determine whether they are associated with an actual source or whether they are a consequence of the reference choice. Furthermore, for modest values of N ($>$30) the loss of this single degree of freedom does not appear to have a significant impact on the potential performance of the LCMV method. The derivation and discussion that follows is applicable whether or not the data is preprocessed to be reference free. For ease of exposition we use $\mathbf{x}$ and $\mathbf{H}(\mathbf{q})$.

III. Linearly Constrained Minimum Variance Localization

The LCMV approach is based on the concept of spatial filtering. Spatial filtering refers to discrimination of signals on the basis of their spatial location. This concept completely parallels the more familiar temporal filtering, where one discriminates between signals based on their temporal frequency content. Hence, a "narrowband" spatial filter passes signals originating from a small "passband" volume while attenuating those originating from other locations. Temporal filtering involves operating on time samples of a signal; spatial filtering involves processing spatial samples of a signal. In the present application, the spatial samples are elements of the data vector $\mathbf{x}$ and the spatial filter is implemented as a weighted combination of these samples. The goal is to design a bank of spatial filters where each filter passes signals originating from a specified location within the brain while attenuating signals from other locations. A display of the variance or power at the output of each filter as a function of the filter's spatial "passband" location provides an estimate of the distribution of activity within the brain.

A. Filter Design

The signal at each location in the brain consists of the three component dipole moment. Hence, we construct three spatial filters for each location, one for each component of the dipole moment. Define the spatial filter for the narrowband volume element Q_o centered on location $\mathbf{q}_o$ as the $N\times 3$ matrix $\mathbf{W}(\mathbf{q}_o)$ and let the three component filter output $\mathbf{y}$ be the inner product of $\mathbf{W}(\mathbf{q}_o)$ and $\mathbf{x}$

$$\mathbf{y} = \mathbf{W}^T(\mathbf{q}_o)\mathbf{x}. \tag{11}$$

An ideal narrowband spatial filter satisfies

$$\mathbf{W}^T(\mathbf{q}_o)\mathbf{H}(\mathbf{q}) = \begin{cases} \mathbf{I} & \mathbf{q} = \mathbf{q}_o \\ \mathbf{0} & \mathbf{q} \neq \mathbf{q}_o \\ & \mathbf{q} \in \Omega \end{cases} \tag{12}$$

where Ω represents the volume of the brain. If (12) is satisfied, then in the absence of noise ($\mathbf{n} = \mathbf{0}$) the filter output is $\mathbf{y} = \mathbf{m}(\mathbf{q}_o)$, the dipole moment at the location of interest.

As in temporal filtering, it is generally impossible to have complete attenuation in the stop band. Unit response in the pass band is insured by requiring

$$\mathbf{W}^T(\mathbf{q}_o)\mathbf{H}(\mathbf{q}_o) = \mathbf{I}. \tag{13}$$

Zero response at any point $\mathbf{q}_s$ in the stop band implies $\mathbf{W}(\mathbf{q}_o)$ must also satisfy

$$\mathbf{W}^T(\mathbf{q}_o)\mathbf{H}(\mathbf{q}_s) = \mathbf{0}. \tag{14}$$

Provided $N \geq 6$ and the columns of $\mathbf{H}(\mathbf{q}_o)$ and $\mathbf{H}(\mathbf{q}_s)$ are linearly independent, it is mathematically possible to simultaneously satisfy (13) and (14). However, if $\mathbf{H}(\mathbf{q}_o)$ and $\mathbf{H}(\mathbf{q}_s)$ are very similar (nearly linearly dependent columns), then $\mathbf{W}(\mathbf{q}_o)$ will have a large norm, resulting in large gain to noise and to sources at locations other than $\mathbf{q}_o$ or $\mathbf{q}_s$. Furthermore, each column of $\mathbf{W}(\mathbf{q}_o)$ only has N degrees of freedom. The pass band constraint (13) uses up three of these, and each independent null uses an additional three so at most one could achieve simultaneous nulls at $N/3-1$ locations having linearly independent transfer matrices $\mathbf{H}(\mathbf{q})$.

Given the limitations on the stopband attenuation, one naturally asks how to design a filter that is optimal in some sense. The LCMV approach offers a guiding philosophy for designing an optimal filter. The idea is to find a $\mathbf{W}(\mathbf{q}_o)$ that minimizes the variance at the filter output while satisfying the linear response constraint (13). Hence, the name linearly constrained minimum variance. The constraints insure that the signals of interest are passed by the filter. Minimization of variance optimally allocates the stop band response of the filter to minimize the contribution to the filter output due to signals in the stop band. This strategy only forces the stopband response to be small at a location $\mathbf{q}_s$ if there is significant energy originating from $\mathbf{q}_s$.

The LCMV problem is posed mathematically as

$$\min_{\mathbf{W}(\mathbf{q}_o)} \operatorname{tr} \mathbf{C}(\mathbf{y}) \text{ subject to } \mathbf{W}^T(\mathbf{q}_o)\mathbf{H}(\mathbf{q}_o) = \mathbf{I}. \tag{15}$$

Alternatively, substituting for $\mathbf{C}(\mathbf{y})$, (15) is expressed as

$$\min_{\mathbf{W}(\mathbf{q}_o)} \operatorname{tr}[\mathbf{W}^T(\mathbf{q}_o)\mathbf{C}(\mathbf{x})\mathbf{W}(\mathbf{q}_o)] \quad \text{subject to } \mathbf{W}^T(\mathbf{q}_o)\mathbf{H}(\mathbf{q}_o) = \mathbf{I}. \tag{16}$$

The solution to (16) may be obtained using the methods of Lagrange multipliers and completing the square. Let $2\mathbf{L}$ be a 3×3 matrix of Lagrange multipliers. The cost function in (16) is augmented with the inner product of the Lagrange multipliers and the constraint to obtain the Lagrangian $L(\mathbf{W}, \mathbf{L})$

$$L(\mathbf{W}, \mathbf{L}) = \operatorname{tr}\left\{\mathbf{W}^T\mathbf{C}\mathbf{W} + (\mathbf{W}^T\mathbf{H} - \mathbf{I})2\mathbf{L}\right\} \tag{17}$$

where the arguments $(\mathbf{q}_o)$ and $(\mathbf{x})$ are omitted for clarity. Noting that $\operatorname{tr}\mathbf{B} = \operatorname{tr}\mathbf{B}^T$ for any square matrix $\mathbf{B}$, we rewrite (17) as

$$L(\mathbf{W}, \mathbf{L}) = \operatorname{tr}\left\{\mathbf{W}^T\mathbf{C}\mathbf{W} + (\mathbf{W}^T\mathbf{H} - \mathbf{I})\mathbf{L} + \mathbf{L}^T(\mathbf{H}^T\mathbf{W} - \mathbf{I})\right\}. \tag{18}$$

It is easy to verify that (18) can be expressed as the perfect square in $\mathbf{W}$

$$L(\mathbf{W}, \mathbf{L}) = \operatorname{tr}\{(\mathbf{W}^T + \mathbf{L}^T\mathbf{H}^T\mathbf{C}^{-1})\mathbf{C}(\mathbf{W} + \mathbf{C}^{-1}\mathbf{H}\mathbf{L}) - \mathbf{L} - \mathbf{L}^T - \mathbf{L}^T\mathbf{H}^T\mathbf{C}^{-1}\mathbf{H}\mathbf{L}\}. \tag{19}$$

Only the first term in the brackets is a function of $\mathbf{W}$. The matrix $\mathbf{C}$ is positive definite so the minimum of $L(\mathbf{W}, \mathbf{L})$ is attained by setting the first term to zero, that is

$$\mathbf{W} = -\mathbf{C}^{-1}\mathbf{H}\mathbf{L}. \tag{20}$$

The Lagrange multiplier matrix $\mathbf{L}$ is now obtained by substituting $\mathbf{W}$ in the constraint $\mathbf{W}^T\mathbf{H} = \mathbf{I}$ to obtain

$$-\mathbf{L}^T\mathbf{H}^T\mathbf{C}^{-1}\mathbf{H} = \mathbf{I} \tag{21}$$

or

$$\mathbf{L}^T = -(\mathbf{H}^T\mathbf{C}^{-1}\mathbf{H})^{-1}. \tag{22}$$

Substituting (22) into (20) yields the solution

$$\mathbf{W}(\mathbf{q}_o) = [\mathbf{H}^T(\mathbf{q}_o)\mathbf{C}^{-1}(\mathbf{x})\mathbf{H}(\mathbf{q}_o)]^{-1}\mathbf{H}^T(\mathbf{q}_o)\mathbf{C}^{-1}(\mathbf{x}). \tag{23}$$

B. LCMV Localization

Using (23) in (11) gives an estimate of the moment at location $\mathbf{q}_o$. The estimated variance or strength of the activity at $\mathbf{q}_o$ is the value of the cost function in (15) and (16) at the minimum. After some algebra we obtain

$$\widehat{\operatorname{Var}}(\mathbf{q}_o) = \operatorname{tr}\left\{[\mathbf{H}^T(\mathbf{q}_o)\mathbf{C}^{-1}(\mathbf{x})\mathbf{H}(\mathbf{q}_o)]^{-1}\right\}. \tag{24}$$

To perform localization, we estimate the variance or strength as a function of location within the volume of the brain. This is accomplished by evaluating (24) as a function of $\mathbf{q}_o$. Regions of large variance presumably have substantial neural activity, while regions with small variance can be considered inactive. We refer to (24) as the estimated "spatial spectrum" of the neural activity. It corresponds to the multiple window minimum variance spectrum estimator described in [16].

This approach does not assume that all sources of activity in the brain are represented by equivalent dipoles, but rather that any source can be explained as a weighted combination of dipoles. Hence, the geometry of sources is not restricted to points, but may be distributed in nature. The source distribution is directly represented by the distribution of significant variance values. Furthermore, this approach does not require specification or determination of the number of dipole sources to fit to the data. Note that anatomical information is easily included by only evaluating (24) at locations corresponding to physically realistic source locations.

The resolution of detail in the spatial spectrum is ultimately limited by the minimum "width" or spatial extent of the filter's passband. Two distinct sources that are located within the passband of a particular filter cannot be resolved. The spatial extent of the passband depends on the transfer matrices $\mathbf{H}(\mathbf{q})$, which in turn depend on the number of electrodes, their distribution, and source location. Simulations indicate that superficial activity can be resolved with much greater detail than deep activity. The resolution also depends on the SNR associated with the feature of interest. This is a consequence of the variance minimization procedure used to determine the spatial filters. As SNR increases, resolution increases. Note that since our analysis is covariance based, SNR is defined as the variance of the source divided by the variance of the noise. This is in contrast to the more usual notion of SNR employed in electroencephalogram (EEG) and evoked potential (EP) analysis, the ratio of the source amplitude to the noise standard deviation.

C. The Neural Activity Index and Noise

The SNR of measured data is often small, so the noise comprises a significant component of the estimated neural activity obtained using (24). Noise that appears spatially concentrated or non uniformly distributed in the spatial spectrum will interfere with localization of actual neural sources. Consider the estimated spatial spectrum assuming $\mathbf{C}(\mathbf{x})$ is due entirely

to uncorrelated noise, $\mathbf{C}(\mathbf{x}) = \mathbf{I}$. In this case, (24) simplifies to

$$\widehat{\mathrm{Var}}(\mathbf{q}_o) = \mathrm{tr}\left\{[\mathbf{H}^T(\mathbf{q}_o)\mathbf{H}(\mathbf{q}_o)]^{-1}\right\}. \tag{25}$$

Hence, the noise spatial spectrum depends on the transfer matrices $\mathbf{H}(\mathbf{q}_o)$. Note that for locations $\mathbf{q}_o$ far from any electrode, the elements of $\mathbf{H}(\mathbf{q}_o)$ are generally quite small, so $[\mathbf{H}^T(\mathbf{q}_o)\mathbf{H}(\mathbf{q}_o)]^{-1}$ will have large elements, resulting in a large value for $\widehat{\mathrm{Var}}(\mathbf{q}_o)$. In contrast, for locations $\mathbf{q}_o$ close to an electrode, $\mathbf{H}(\mathbf{q}_o)$ will have several large elements and $[\mathbf{H}^T(\mathbf{q}_o)\mathbf{H}(\mathbf{q}_o)]^{-1}$ will have generally have small elements, resulting in a small value for $\widehat{\mathrm{Var}}(\mathbf{q}_o)$. Because deep source locations are relatively far from electrodes, noise generally has a dome shaped spatial spectrum with the peak of the dome centered at the deepest locations. This dome may be warped significantly if the electrodes are distributed nonuniformly, or if the geometry of the head is assumed to be very nonuniform.

The LCMV spatial spectrum is not linear, that is, the spatial spectrum due to a sum of signals is not the sum of the individual spatial spectra. This is a consequence of the inverses in (24). However, application of the matrix inversion lemma[1] to (6) and substitution into (24) indicates that (24) always contains an additive noise component of the form

$$\mathrm{tr}\left\{[\mathbf{H}^T(\mathbf{q}_o)\mathbf{Q}^{-1}\mathbf{H}(\mathbf{q}_o)]^{-1}\right\}. \tag{26}$$

This corresponds to the noise spatial spectrum in the absence of other signals. Due to the relatively low SNR's associated with typical data, the noise spatial spectrum may obscure the spatial spectrum of the neural activity of interest. This problem is reduced by normalizing the estimated spatial spectrum of the data by the estimated noise spatial spectrum to obtain the normalized estimate

$$\widehat{\mathrm{Var}}_N(\mathbf{q}_o) = \frac{\mathrm{tr}\left\{[\mathbf{H}^T(\mathbf{q}_o)\mathbf{C}^{-1}(\mathbf{x})\mathbf{H}(\mathbf{q}_o)]^{-1}\right\}}{\mathrm{tr}\left\{[\mathbf{H}^T(\mathbf{q}_o)\mathbf{Q}^{-1}\mathbf{H}(\mathbf{q}_o)]^{-1}\right\}}. \tag{27}$$

We term this estimate the neural activity index.

The numerator of (27) is an estimate of the source plus noise variance at $\mathbf{q}_o$ and the denominator is an estimate of the noise variance at $\mathbf{q}_o$; hence, the neural activity index may be interpreted as an estimate of the source to noise variance as a function of location. The normalization is a function of location so the relative levels of estimated neural activity at different locations is changed. In principle, the absolute level can still be determined by reversing the normalization after specific features are identified.

The neural activity index requires knowledge the noise covariance matrix $\mathbf{Q}$. $\mathbf{Q}$ may be estimated from data that is known to be source free, such as pre stimulus data in a EP's experiment. Alternatively, if the noise is assumed uncorrelated between channels, then $\mathbf{Q} = \mathbf{I}$. Note that the absolute level of the noise is not required, it is only the shape or form of the noise covariance that is needed. Changing the absolute level modifies the entire estimate by a common constant.

[1]The matrix inversion lemma states that if $\mathbf{A}$ and $\mathbf{B}$ are two positive definite $M \times M$ matrices related by $\mathbf{A} = \mathbf{B} + \mathbf{C}\mathbf{D}\mathbf{C}^T$, where $\mathbf{D}$ is another positive definite $N \times N$ matrix and $\mathbf{C}$ is an $M \times N$ matrix, then $\mathbf{A}^{-1} = \mathbf{B}^{-1} - \mathbf{B}^{-1}\mathbf{C}(\mathbf{D}^{-1} + \mathbf{C}^T\mathbf{B}^{-1}\mathbf{C})^{-1}\mathbf{C}^T\mathbf{B}^{-1}$.

D. Correlated Sources

Recall that the moments associated with distinct dipoles were assumed to be uncorrelated [see (4)]. The presence of correlation between distinct sources can lead to reduction of the estimated variance for the sources that are correlated.

Letting

$$\mathbf{C}(\mathbf{q}_i, \mathbf{q}_j) = E\{[\mathbf{m}(\mathbf{q}_i) - \overline{\mathbf{m}}(\mathbf{q}_i)][\mathbf{m}(\mathbf{q}_j) - \overline{\mathbf{m}}(\mathbf{q}_j)]^T\} \tag{28}$$

be the cross covariance between sources at $\mathbf{q}_i$ and $\mathbf{q}_j$, the output variance at location $\mathbf{q}_k$ is given as

$$\begin{aligned}
&\mathrm{tr}\left\{\mathbf{W}^T(\mathbf{q}_k)\mathbf{C}(\mathbf{x})\mathbf{W}(\mathbf{q}_k)\right\} \\
&= \mathrm{tr}\left\{\mathbf{C}(\mathbf{q}_k) + \sum_{\substack{i=1\\ i\neq k}}^{L} \mathbf{W}^T(\mathbf{q}_k)\mathbf{H}(\mathbf{q}_i)\mathbf{C}(\mathbf{q}_i)\mathbf{H}^T(\mathbf{q}_i)\mathbf{W}(\mathbf{q}_k)\right. \\
&\quad + \sum_{\substack{i=1\\ i\neq k}}^{L} \mathbf{C}(\mathbf{q}_k, \mathbf{q}_i)\mathbf{H}^T(\mathbf{q}_i)\mathbf{W}(\mathbf{q}_k) \\
&\quad + \mathbf{W}^T(\mathbf{q}_k)\mathbf{H}(\mathbf{q}_i)\mathbf{C}(\mathbf{q}_i, \mathbf{q}_k) \\
&\quad + \sum_{\substack{n,i=1\\ n,i\neq k\\ n\neq i}}^{L} \mathbf{W}^T(\mathbf{q}_k)\Big[\mathbf{H}(\mathbf{q}_i)\mathbf{C}(\mathbf{q}_i, \mathbf{q}_n)\mathbf{H}^T(\mathbf{q}_n) \\
&\qquad\qquad + \mathbf{H}(\mathbf{q}_n)\mathbf{C}(\mathbf{q}_n, \mathbf{q}_i)\mathbf{H}^T(\mathbf{q}_i)\Big]\mathbf{W}(\mathbf{q}_k) \\
&\quad \left. + \mathbf{W}^T(\mathbf{q}_k)\mathbf{Q}\mathbf{W}(\mathbf{q}_k)\right\}.
\end{aligned} \tag{29}$$

Here, we have used $\mathbf{W}^T(\mathbf{q}_k)\mathbf{H}(\mathbf{q}_k) = \mathbf{I}$ to simplify (29). The cross terms in the second through fifth lines on the right-hand side of (29) are not guaranteed to be positive for all $\mathbf{W}(\mathbf{q}_k)$. Recall that the LCMV criterion chooses a $\mathbf{W}(\mathbf{q}_k)$ to minimize (29). The minimum is generally obtained with a $\mathbf{W}(\mathbf{q}_k)$ that would make the cross terms in the second through fifth lines negative. If this occurs, then the estimated variance of the source at $\mathbf{q}_k$, $\mathrm{tr}\left\{\mathbf{W}^T(\mathbf{q}_k)\mathbf{C}(\mathbf{x})\mathbf{W}(\mathbf{q}_k)\right\}$, is significantly less than its true value, $\mathrm{tr}\left\{\mathbf{C}(\mathbf{q}_k)\right\}$. The spatial filter exploits the correlation between sources to minimize output variance by canceling the correlated portion of the source of interest. Correlated source cancellation is a phenomenon that is well known in adaptive beamforming applications of the LCMV method for radar and sonar [23].

Perfect correlation between spatially distinct sources in the brain is unlikely, although partial correlation is expected in certain situations, such as when several brain areas react to an external stimulus or become activated by a common third active area. We explore the performance of the LCMV method in the presence of correlated source activity in the simulation section. The results indicate that the method is robust to moderate levels of correlation between sources.

IV. Estimating the Covariance Matrix

The spatial spectrum estimate (24) and neural activity index (27) require knowledge of the data covariance matrix $\mathbf{C}(\mathbf{x})$.

In practice, $\mathbf{C}(\mathbf{x})$ is unknown and must be estimated from the available data. One estimate is the sample covariance matrix

$$\hat{\mathbf{C}}(\mathbf{x}) = \frac{1}{M-1} \sum_{n=1}^{M} (\mathbf{x}_n - \overline{\mathbf{x}})(\mathbf{x}_n - \overline{\mathbf{x}})^T \tag{30}$$

where

$$\overline{\mathbf{x}} = \frac{1}{M} \sum_{n=1}^{M} \mathbf{x}_n \tag{31}$$

is the sample mean and $\mathbf{x}_n$, $n = 1, 2, \cdots, M$ are observations of the phenomena to be localized. Note that these observations must all correspond to the same underlying spatial spectrum, that is, the data must be wide sense stationary. If the data set contains observations associated with different spatial spectra, the estimated spatial spectrum derived using the covariance estimate (30) will correspond to a mixture of the underlying spatial spectra.

The number of observations M must at minimum exceed the number of elements in each data vector, N, for $\hat{\mathbf{C}}(\mathbf{x})$ to be nonsingular. Since $\hat{\mathbf{C}}(\mathbf{x})$ is constructed from random data, it is a random quantity. Randomness in $\hat{\mathbf{C}}(\mathbf{x})$ will introduce randomness into the estimated spatial spectrum. Excessive randomness may obscure features of interest or result in false recognition of nonexistent sources. This randomness decreases as M increases. Statistical analyzes assuming independent Gaussian distributed observations for related problems [16], [24] have shown that for a given true covariance matrix the ratio of M to N determines the randomness in the estimated spatial spectrum. A common rule of thumb in such problems is to choose M several times as large as N. Hence, if $N = 100$ electrodes are used, then on the order of 300–400 independent observations should be used to construct $\hat{\mathbf{C}}(\mathbf{x})$

This guideline may be difficult to satisfy in some applications. For example, in some patients it may be difficult to identify several hundred epileptic spikes. An alternative is to use multiple observations or samples in time from each single event, such as a spike, to construct $\hat{\mathbf{C}}(\mathbf{x})$. In this approach the variability used for localization is due in part to the time variation of the event. If multiple samples in time are used to construct the covariance matrix, then one must assume that the data is wide sense stationary over the time interval, that is, that all data is associated with the same underlying spatial spectrum. A second concern with using multiple time samples is possible reductions in the degree of statistical independence between adjacent observations. Any statistical dependence will increase the number of observations needed to maintain comparable levels of randomness in the covariance matrix estimate.

If multiple observations of an event are available and the data is temporally stationary, then one can ask whether the best performance is obtained using time samples of an averaged event or using time samples of all observations to estimate the covariance matrix. The answer to this question is complex and in general requires complete statistical characterization of neural activity. A significant factor is the relative variability of the noise to that of signal or sources over both time and from observation to observation. Averaging procedures reduce both the variance associated with sources and the variance associated with the noise. If the decrease in noise variance obtained by averaging is greater than the decrease in signal variance, then averaging is advantageous. For example, if the signal variability is primarily over time and not from one observation to another, then at low SNR averaging improves performance since it reduces the noise variability but does not decrease the temporal variability of the signal. A less-significant factor is the reduced the number of data vectors available for estimating the covariance matrix when averaging is used. With fewer data vectors the randomness in the covariance matrix estimate would tend to increase. However, averaging also changes the underlying true data covariance matrix by reducing the noise component, an effect that tends to reduce the randomness in the estimated covariance matrix.

Our simulations demonstrate that the LCMV approach is effective when the primary variability is over time or from one observation to another (see Section V-D). The method for determining the estimated covariance matrix may be changed to exploit the underlying mechanism for signal and noise variability.

V. Examples

Intuitively, one might assume that the quality of the results obtained with the spatial filtering approach is determined by a number of factors including the SNR of the measurements, the number and distribution of sensors, and in general the match between the assumptions in the model and reality. In this section, we explore the results obtained by the spatial filtering method when some of the parameters are varied and certain assumptions are partially violated. To exclude the effects of model geometry and allow for quantitative control of certain variables, we study the effects in a number of simulations where the measurements and the transfer function are generated with the same model. Other parameters such as signal-to-noise, electrode positions, and number of electrodes are kept close to realistic values. The performance under realistic conditions is evaluated using data collected from a patient with implanted depth electrodes.

The physical model for the head is a three-shell sphere. The outer shell models the skin, the middle shell represents the skull surrounding the centrally located brain tissue. The surface potential of the outer layer was calculated with the algorithm described in [6]. With the exception of the simulations with variable reference electrode, all simulations assume a reference at an infinite distance with zero potential. The electrode locations are determined by mapping standard 10–20 system plus extended positions [25] onto a spherical head. The outer radius of the assumed head is 8.25 cm; the middle and outer shells are 0.3-cm and 0.7-cm thick, respectively. The conductivity ratio between bone and soft tissue is 0.0125. The transfer matrices $\mathbf{H}(\mathbf{q})$ are calculated for horizontally located cross sections at 1-cm intervals. In each of the sections, transfer functions are determined on a uniform grid with 0.25-cm spacing in each direction. The neural activity index landscape and contour plots represent horizontal cross sections of the head. The vertical location of each cross section is represented by a position on a Z-axis, with increasing height

corresponding to increasing Z values. Within each cross section the X-axis is front–back with front positive and the Y-axis is right–left with left positive.

A. Neural Activity Index and Electrode Distribution

In many laboratories, the distribution of the recording electrodes is adapted to the assumed localization of the neural dysfunction. As described in Section III-C, the noise distribution is related to electrode positions. For this reason, we evaluate performance of the algorithm with different 32-channel electrode montages: one with a homogeneous electrode distribution and the other with all electrodes on one half of the sphere. In the homogeneous distribution the selection is: Fp1, Fp2, AF3, AF4, F7, F3, Fz, F4, F8, FC5, FC1, FC2, FC6, T3, C3, Cz, C4, T4, CP5, CP1, CP2, CP6, T5, P3, Pz, P4, T6, PO3, PO4, O1, Oz, O2; the other distribution contains only frontally located positions: Fp1, Fpz, Fp2, AF7, AF3, AFz, AF4, AF8, F7, F5, F3, F1, Fz, F2, F4, F6, F8, FT7, FC5, FC3, FC1, FCz, FC2, FC4, FC6, FT8, T9, T3, C5, C3, C1, Cz.

The noise spatial spectrum computed using (24) in the horizontal section at the center of the sphere ($Z = 0$ cm) is shown in Fig. 1. The covariance matrix represents white noise $[\mathbf{C}(\mathbf{x}) = \mathbf{I}]$. The result for the symmetrical electrode positions [Fig. 1(a)] shows a dome shaped noise distribution, while the frontally located electrode distribution generates more noise in the occipital area [Fig. 1(b)]. In cases with a low SNR this montage dependent noise distribution presents a problem since it may obscure actual sources. For this reason, we normalize the spatial spectrum by the noise spatial spectrum to obtain the neural activity index (27). The neural activity indexes for both montages are identical, and depicted in Fig. 1(c).

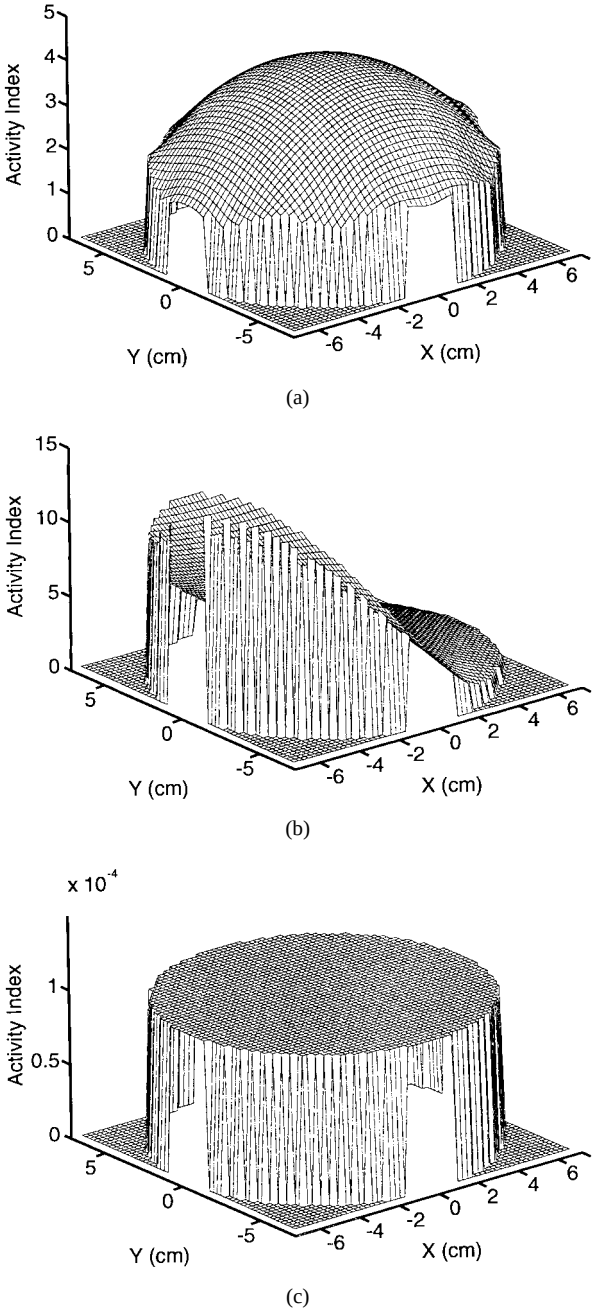

Fig. 1. The relationship of electrode distribution to the noise spatial spectrum. In (a) and (b), the noise spatial spectrum is depicted in the horizontal cross section (XY plane) through the center of a spherical head model. In case (a) the electrodes are distributed homogeneously over the spherical surface. The resulting spatial spectrum is characterized by a dome shape. In (b), the electrodes were located in a set on one side. The maximum spatial spectrum is found on the side of the head opposite the electrode set. Electrode location dependent differences in the noise spatial spectrum are equalized by computing a neural activity index (27). The result of this normalization is shown in (c).

B. Dependence on Reference Choice

Choice of reference electrode is always an issue in clinical neurophysiology. One is most likely to detect activity standing out against the background when the signals are recorded with a reference that is remote. If the reference is close to the activity, the signal will appear in all recorded channels and prevent easy localization based on visual inspection.

We simulated several cases in which we evaluated spatial filter output having a pair of sources separated by 3 cm at a depth of 0.75 cm from the surface of the inner sphere and located in a horizontal section at $Z = 1$ cm. The SNR (variance) was set at 9.5. We evaluated three different situations: 1) reference at infinity; 2) reference being the closest positioned electrode; 3) using the most remotely located electrode as the reference. The homogeneous 32-channel montage described in the previous subsection was employed. The neural activity index varied only slightly; the sources were detected in the correct locations in all three cases. In the different situations, the maximum values of the neural activity index varied by only 10%. The largest difference was found between the close reference and the two other situations; with the close reference resulting in a higher peak value. The landscapes of the neural activity index plotted on a relative scale were very similar in all three cases. Minor differences in the landscape can only be detected by superimposing the plots.

C. Correlated Sources

We previously noted that correlation between sources may lead to degraded algorithm performance. For this reason, we examined the effect of uncorrelated, partially correlated and completely correlated source activity in two different

simulations, one with two sources having a small interdistance and another with two sources having a large interdistance. The sources are located in the inner sphere at $Z = 1$ cm: the close sources have X, Y coordinates of 1.375, -6.375, and -1.625, -6.375; the distant sources have X, Y coordinates of 1.375, 6.375, and 1.375, -6.375. The correlation between the sources was varied by assuming the dipole moments $\mathbf{m}_1$ and $\mathbf{m}_2$ were related by

$$\mathbf{m}_1 = \alpha \mathbf{m}_2 + \boldsymbol{\nu}. \tag{32}$$

Here, α determines the degree of correlation between the sources and $\boldsymbol{\nu}$ represents the uncorrelated component. We considered cases in which the sources are uncorrelated ($\alpha = 0$), partially correlated ($\alpha = 0.5$), and completely correlated ($\alpha = 1$). The uncorrelated component was adjusted in each case to obtain a SNR of ten.

The result of these simulations is shown in Fig. 2. The first column of landscape plots [Fig. 2(a)–(c)] shows the effects of correlation for the closely spaced dipoles. In the uncorrelated case the two peaks can be distinguished clearly [Fig. 2(a)]. With moderate correlation increases the peaks start to merge [Fig. 2(b)] and in the fully correlated case [Fig. 2(c)] only one peak located in the middle is evident. For remote sources the result is somewhat different. The noncorrelated situation generates two distinct peaks in the landscape of the neural activity index [Fig. 2(d)]. As illustrated in Fig. 2(e), partial correlation decreases the height of each peak, but still allows detection of the dipole locations. Fully correlated distant sources have a tendency to cancel each other in the neural activity index [see Fig. 2(f), note that the scale has changed].

D. Covariance Matrix Estimation—Mean and Variance

A major difference between this method and most currently available techniques is the use of (co)variance instead of signal amplitude. As described previously, the covariance matrix can be estimated in different ways. One can use observations from a recording at time instants that one believes are comparable; e.g., peaks in different spikes or EP responses. Alternatively, if one has reason to believe that a certain area is active over a given time interval, one can select a sequence of sampled points. Both approaches can also be combined by selecting a window of measured values over comparable epochs in a signal. In each case, we assume the observations used to estimate the covariance matrix represent brain activity at the same locations.

We used simulations to examine the efficacy of different approaches for selecting the observations used to estimate the covariance matrix. A single dipole at $X = 1.375$ cm, $Y = -6.375$ cm, and $Z = 1$ cm was used to generate data for the homogeneous 32-channel montage described previously. The source consisted of a dipole moment whose time variation is represented by 75 samples taken from one cycle of a sinusoid plus a random component. Noise was added to obtain a SNR of approximately ten. Two different situations are considered: one in which the sinusoidal amplitude variation contributes 20% of the total source power and a second in which the sinusoidal amplitude variation represents 80% of the total source power. The random component of the source generates the remaining power. In each of the situations we generated 75 repetitions. Three different techniques were used to estimate the covariance matrix from the 75 repetitions of the 75 time points: 1) using all 75 time points of all 75 repetitions; 2) using a single time point (the fifth) in the 75 repetitions; and 3) using all 75 time points after averaging the 75 repetitions.

The results of the simulation are shown in Fig. 3. Fig. 3(a)–(c) represents the results for the dipole with a relatively high amplitude, and Fig. 3(d)–(f), the dipole with a high variance component. The first row of Fig. 3 [(a), (d)] depicts the results when all time points of all repetitions are used to estimate the covariance matrix. In this case, there is no difference between the high amplitude and high variance cases. Use of a single observation gives best results when the signal has a high variance component as illustrated in Fig. 3(e). Estimating the covariance matrix from the average of the repetitions works best with the large amplitude component case, although excellent results are also obtained in the high variance case [Fig. 3(c) and (f)].

E. Localization of Stimulus Electrode Positions in the Brain

The simulations presented thus far use the same model geometry to generate the data and the transfer matrices. This facilitates examination of effects that cannot be controlled or measured in a realistic situation. However, in a realistic situation the modeled geometry is only an approximation to the actual geometry. We now explore the sensitivity of the method to deviations between actual and assumed geometry by using actual neurophysiological data. This implies we must relate the locations of sources identified in our spherical model to their actual location in the human head. In most neurophysiological recordings, the real source location(s) is/are unknown. Recorded data can be used to verify localization algorithms only in unusual cases. The best example of such exceptional data is where the source is artificially planted in the brain.

We obtained this type of data from a patient that had a possibility of epilepsy after craniotomy for clipping an intracranial aneurysm. Electrodes were inserted during craniotomy and used to monitor EEG after surgery. Stimulation was performed with informed consent of the patient. A stimulus pulse was delivered between different sets of electrodes to induce neural activity. One series of pulses were delivered between the two most "proximal" electrodes (set 1); the other between the most "distal" pair (set 2). The X rays from a lateral and fronto-dorsal view are shown in Fig. 4(a) and (b). The position of set 1 is medial, slightly occipital and approximately 1 cm lower than set 2. The EEG and stimulus pulse were measured using only 20 channels (the 10–20 positions plus Oz) with linked ears as a reference; the data was amplified by 20 000 and filtered to pass components between 1 and 90 Hz. As can be seen in the example of set 1 data depicted in Fig. 4(c), the amplitude of the generated signal is slightly higher than the surrounding EEG; a situation comparable to an epileptic spike. To remove signals from other EEG sources, the data was highpass filtered at 40 Hz; the result shown in Fig. 4(d). Nineteen samples from seven pulses were used to estimate the covariance matrix.

The contour plots of the neural activity index for sets 1 and 2 are shown in Fig. 4(e) and (f). The peaks associated with

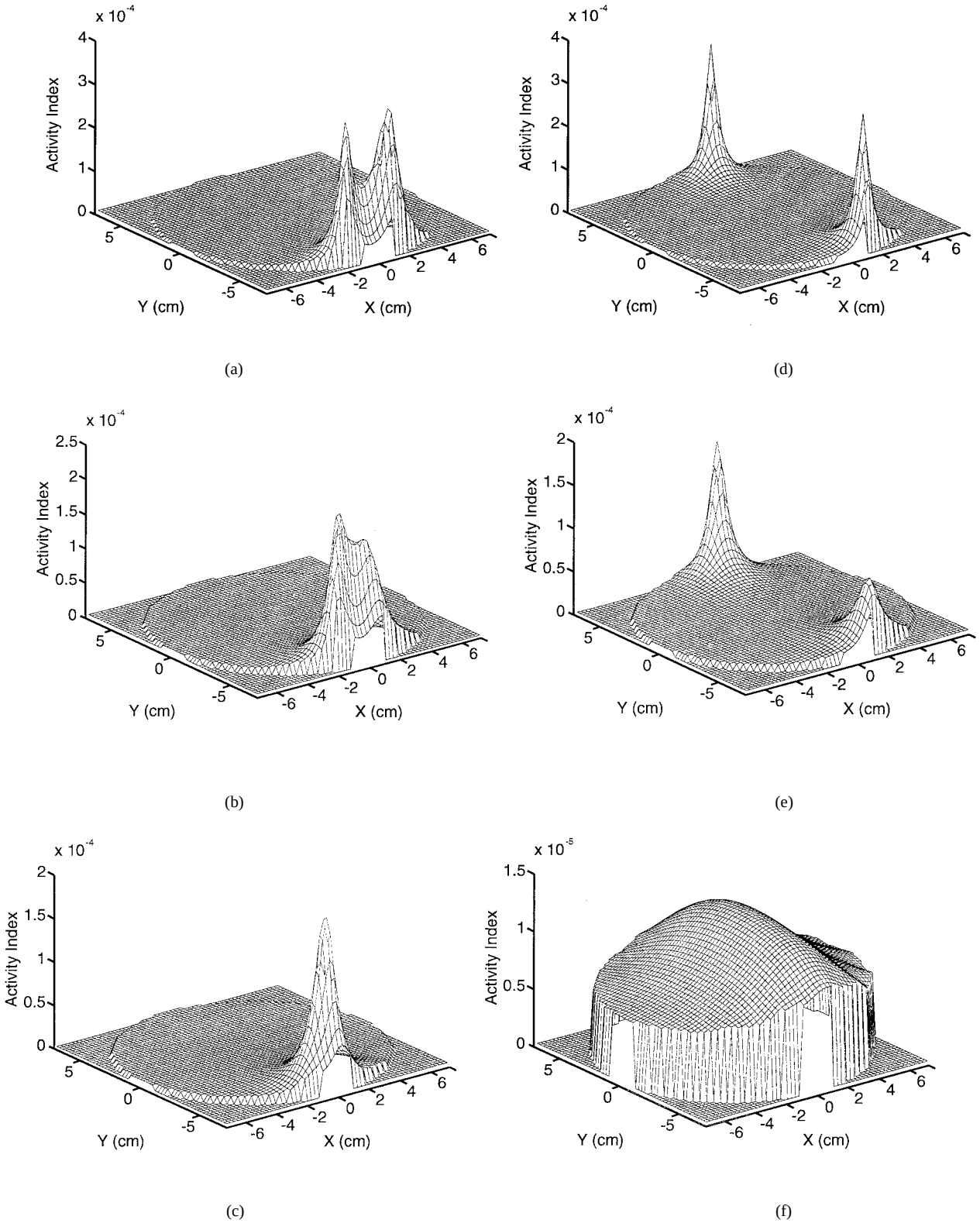

Fig. 2. The effect of correlation between sources on the neural activity index. The two correlated sources are closely spaced in (a)–(c) and relatively distant in (d)–(f). The sources are uncorrelated in (a) and (d), partially correlated in (b) and (e), and fully correlated in (c) and (f). Sources can be detected from the distribution of peaks in the neural activity index provided some uncorrelated activity is present [(a), (b), (d), and (e)]. When the sources are fully correlated it is no longer possible to detect distinct source locations [(c) and (f)]. Sources that are closely spaced tend to merge (c), while the distant sources nearly completely cancel each other (note the scale differences between the plots).

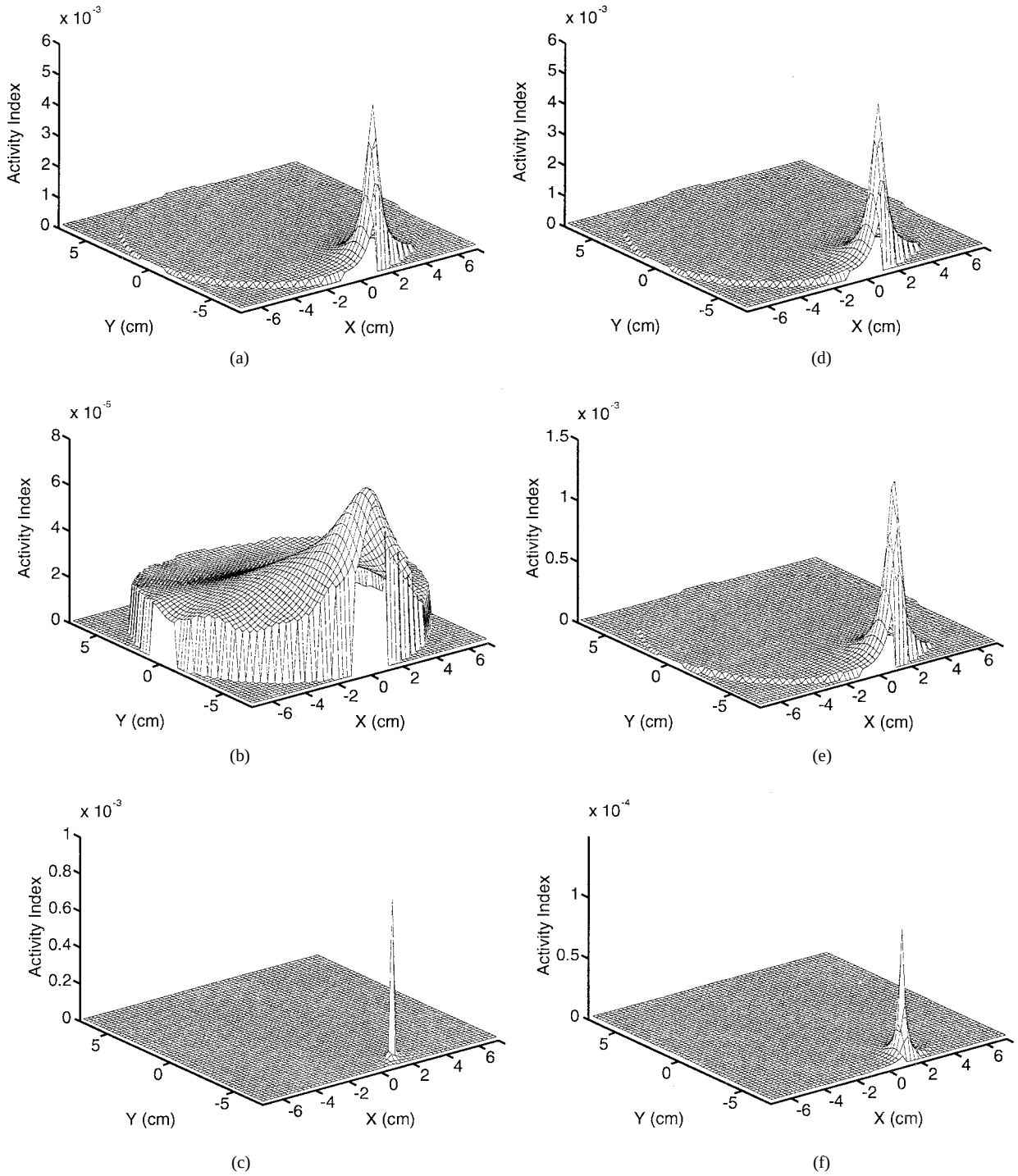

Fig. 3. The effect of using different estimates of the covariance matrix. The neural activity index in a horizontal section 1cm above the center of the sphere is depicted. The dipole moment of the source has a repeatable sinusoidal component plus a random component. In (a)–(c), 80% of the activity is the repeatable component and 20% random. In (d)–(f), the repeatable component is 20% with 80% random. The data consist of 75 time points from 75 trials. In (a) and (d) the covariance matrix is estimated using the entire data record, in (b) and (d) a single time point in each trial is used, while in (c) and (e) the 75 time points in the average over the trials is used. The scale of the neural activity index is adjusted in each case. There is no difference between the primarily repeatable and the primarily random case [(a), (d)] when the entire data set is employed. Selecting a single point in each trial works best if the source is primarily random (e). Averaging reduces the trial to trial variability in the source as well as the noise and gives the best result when the source is dominated by a repeatable component (c), although excellent results are obtained in the random component case (f), since averaging does not reduce the source randomness within the trial.

the sources are relatively diffuse due to the limited resolution available with only 20 electrodes. The superficially located peak associated with set 2 is sharper than the peak associated with the deeper activity in the set 1 data. Measurements necessary to register the source locations indicated on the X ray with the coordinates of our spherical head model were not available, so we compare the relative positions of the actual and estimated sources to the 10–20 system electrode locations. The correspondence is very good. Viewed laterally on a Front-Back axis, the sources are located between the

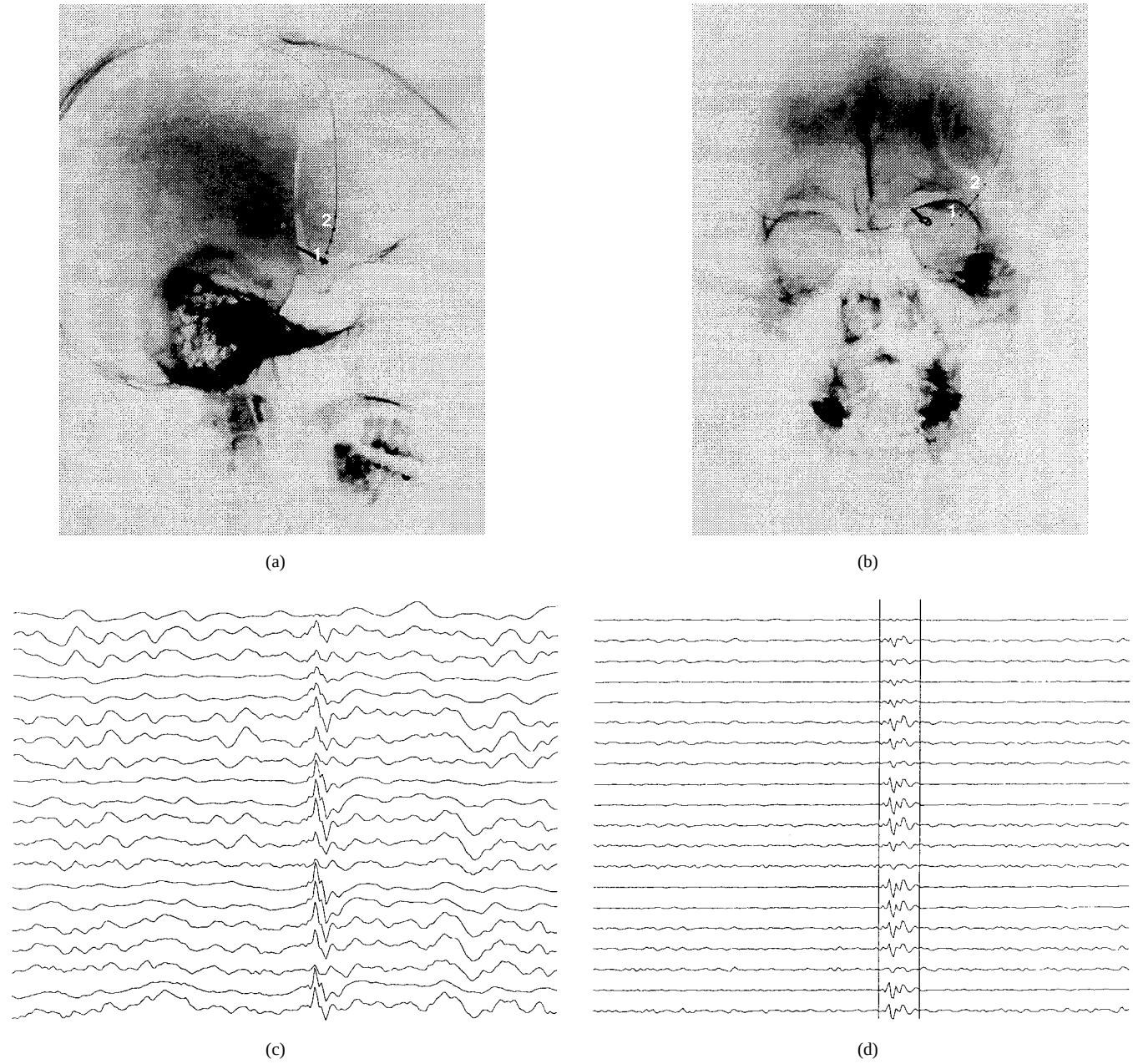

Fig. 4. Localization of stimulus electrodes implanted in the brain. The electrode positions within the brain are shown in lateral view (a) and frontal view (b) X-ray images. The stimulus electrodes for set 1 are lower, somewhat more medial and occipital than the set 2 electrodes. (c) Example of the data generated in response to stimulus of electrode pair set 1. (d) The solution is based on a spherical model. The maximum activity in set 1 is found 1 cm below the center of the sphere while the set 2 maximum is located 1 cm higher. The relative positions of the maxima and the position of each maxima relative to the surface electrode positions agree well with the anatomical positions of the stimulus electrodes.

temporal (T4) and frontal (F8) electrodes. On an Up-Down axis the set 1 and set 2 sources are slightly below and above the temporal electrodes (T4), respectively. In the frontal plane on a right–left axis, both sources are on the right side; set 2 close to the line that connects Fp2 and O2. The relative positions of the set 1 and set 2 sources are also as expected: the set 1 source is found deeper, more medial and occipital than the set 2 source.

VI. Discussion

The LCMV spatial filtering method described herein is attractive because one does not have to determine the number of active sources *a priori*. The requirement of knowing the number of active sources *a priori*, or estimating the number from the data is a major limitation in most proposed source localization algorithms, for example [1], [5], [7], [8], [10], [26], and [27]. When the number of estimated sources is less than the true number of active areas such algorithms will typically detect resultant activity somewhere in between the actual areas. A trivial example of such a mislocalization is single dipole localization performed on bilateral somatosensory stimulation. Both hemispheres are active from approximately 20 ms after bilateral stimulation of the wrist. However, it is well known that single dipole analyzes performed on the so

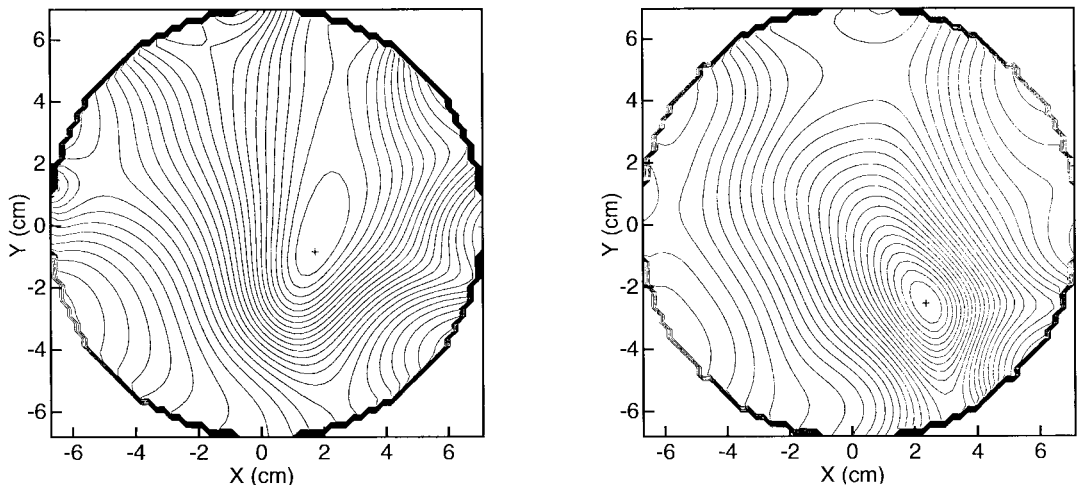

(e) (f)

Fig. 4. (*Continued.*) Localization of stimulus electrodes implanted in the brain. Contour plots of the neural activity index in a horizontal cross section are shown in (e) (set 1) and (f) (set 2). The solution is based on a spherical model. The maximum activity in set 1 is found 1 cm below the center of the sphere while the set 2 maximum is located 1 cm higher. The relative positions of the maxima and the position of each maxima relative to the surface electrode positions agree well with the anatomical positions of the stimulus electrodes.

called N20 yield a resultant source whose anatomical correlate is the medial fissure between the hemispheres. In this example, the error is easy to correct by assuming two active areas. In many other situations such an easy correction is not feasible because an educated guess of the number of active areas cannot be made. The examples in Section V and [22] illustrate that distinct peaks in the neural activity index can actually indicate the number of sources under certain conditions.

The localization technique presented here is closely related to the adaptive filtering approach of Spencer *et al.* [21]. They describe a method for monitoring the time series associated with a component of a current dipole source vector at a given location. An LCMV criterion is used to determine the adaptive filter coefficients, resulting in an expression equivalent to (23). Synthetic data is used to illustrate the potential effectiveness of the approach.

Our work is also related to that of Dale and Sereno [12]. First of all, they also employ covariance information for localization, assuming sources are zero mean. Second, they estimate the dipole strength as a function of location using a linear function of the sensor data. However, instead of using an LCMV criterion to find the linear operator, they minimize the expected error between the estimated and actual solution. The linear operator is then dependent on the dipole and noise covariance matrices which are unknown. They propose either assuming a form for these covariance matrices *a priori,* or attempt to estimate them from the sensor covariance. The dipole variance is estimated using a modification of the multiple signal classification (MUSIC) algorithm [10] in which the projection of gain vectors onto each eigenvector is weighted by the reciprocal of the corresponding eigenvalue. The gain vector is determined from the transfer matrix $\mathbf{H}(\mathbf{q})$ and *a priori* knowledge of the dipole orientation. The functional form of the neural activity index (27) is similar to their modification of the MUSIC algorithm in the special case $\mathbf{Q} = \mathbf{I}$. We do not presuppose knowledge of the dipole orientation and thus the neural activity index depends on all columns of $\mathbf{H}(\mathbf{q}_o)$ rather than a gain vector.

The LCMV approach is easily modified to incorporate prior knowledge of dipole orientation. Let $\mathbf{a}(\mathbf{q}_o)$ be the gain vector associated with a dipole at location $\mathbf{q}_o$. We now design a single spatial filter $\mathbf{w}(\mathbf{q}_o)$ to minimize output variance subject to a unit gain constraint on the response to the dipole of interest, resulting in the LCMV problem

$$\min_{\mathbf{w}(\mathbf{q}_o)} \mathbf{w}^T(\mathbf{q}_o)\mathbf{C}(\mathbf{x})\mathbf{w}(\mathbf{q}_o) \text{ subject to } \mathbf{w}^T(\mathbf{q}_o)\mathbf{a}(\mathbf{q}_o) = 1.$$

The neural activity index associated with this problem is then

$$\widehat{\mathrm{Var}}_N(\mathbf{q}_o) = \frac{\mathbf{a}^T(\mathbf{q}_o)\mathbf{Q}^{-1}\mathbf{a}(\mathbf{q}_o)}{\mathbf{a}^T(\mathbf{q}_o)\mathbf{C}^{-1}(\mathbf{x})\mathbf{a}(\mathbf{q}_o)}.$$

This corresponds exactly to the MUSIC based variance estimator of Dale and Sereno [12] when $\mathbf{Q} = \mathbf{I}$. Note that our derivation of the neural activity index using principles of spatial filtering offers insight into performance and characteristics that are not evident from the MUSIC-based variance estimator derivation. This variance estimator contains contributions due to the dipole source at $\mathbf{q}_o$, other dipoles that leak through the spatial filter sidelobes, and noise. The effect of these two contaminants on the linear operator used to perform localization in [12] and the ultimate localization performance has not been reported.

As in any approach, the LCMV spatial filtering method described here is developed assuming a model for the underlying neural activity. Our results suggest that the algorithm is robust to many violations of the underlying assumptions.

The effect of correlation between sources is evaluated using analysis and simulations. The simulation results (Fig. 2) indicate that localization of correlated sources is possible as long as some of the source activity is uncorrelated. If there is a high correlation between sources, one may obtain resultant activity in between the real active areas [Fig. 2(c)], similar to the resultant activity in other localization algorithms

associated with under estimation of the number of sources. In our case, the algorithm effectively treats closely spaced correlated sources as a single source. Alternatively, the activity level is generally underestimated if the correlated sources are relatively distant [Fig. 2(f)]. Although some correlation in neural activity in the brain is expected, perfect correlation between spatially disparate is unlikely. Hence, we believe that the partially correlated cases in Fig. 2(b) and (e) are realistic. While partial correlation decreases the estimated activity level, power of the filter output, different sources still may be distinguished given a reasonable SNR and enough electrodes.

The LCMV approach is an attempt to exploit variable features in the data. Neural responses, as all physiological processes, are not perfectly reproducible. The variability in subaverages of an EP and in spike and seizure activity in an electroencephalogram are likely due to both variability in the underlying signal as well as surrounding ongoing activity. The method is robust to the source of variability used for localization, whether epoch to epoch variations or variation over time. This allows considerable flexibility in obtaining data with which to estimate the covariance matrix. For example, in situations with low SNR such as an evoked response, averaging can be used to reduce noise. Averaging also reduces signal epoch to epoch variability, but will not reduce the temporal variation associated with the repeatable component of the response. This temporal variation can be used for localization by estimating the covariance matrix with temporal samples. We have illustrated the effect of using epoch to epoch variability and temporal variability to estimate the covariance matrix in simulations by varying the relative contributions of source amplitude and variance (Fig. 3). In general, the best method for estimating the covariance matrix depends on the source's relative components of temporal and epoch to epoch variability and the noise statistics.

We have assumed that the data used to estimate the covariance matrix results from a stationary source distribution. If different source distributions are represented in the covariance matrix, the neural activity index will represent a combined activity pattern. For example, suppose one source is active in the first part of the data and two others are active in the second part. The neural activity index based on the combined data will in general indicate three active sources. If many active areas are present, the neural activity index will likely indicate a broad region of activity and individual sources will not be evident. The method cannot resolve differences in the underlying activity distributions once the corresponding data is combined into a single covariance matrix estimate. Determining whether a data set corresponds to a stationary spatial source distribution is beyond the scope of the present work. One may assume that similar areas of the brain are involved in different subaverages of a EP because the activity is stimulus related. During an epileptic discharge it may be necessary to compare the topography of a series of spikes before concluding that different spikes originate from the same underlying source distribution.

The data generated by implanted electrodes was chosen to have approximately the same order of magnitude as the spontaneous electrical activity [see Fig. 4(c)] in order to approximate a typical epileptic discharge. This assumption on the relative magnitude of an epileptic discharge is supported by data described in van Drongelen *et al.* [22]. The primary purpose of this data set is to demonstrate the methods ability to localize when there are deviations between the actual and assumed head geometry (see Fig. 4). The sources were localized in a diffuse area because only 20 electrodes were used. While increasing the number of electrodes would lead to improved resolving capability, it would also increase the sensitivity to deviations between actual and assumed geometries. High-resolution results when the spatial filter is able to discriminate between signals with subtle differences in their transfer matrices due to location. Modeling errors also lead to subtle differences in transfer matrices. When modeling errors are present, the spatial filtering constraint no longer insures that a source at a given location is passed with unit gain because the actual and modeled transfer matrices differ. If the electrode array has high enough resolution to discriminate between actual and modeled transfer matrices, then the spatial filter will attenuate the source, resulting in underestimation of source power. Hence, the importance of accurate head modeling increases with increasing numbers of electrodes.

In this particular data set, the errors introduced by assuming a spherical model should be minimal because the sources are centrally located. Note that our spatial filtering approach for solving the inverse problem is not limited to a particular head model for solving the forward problem. Indeed, as in most approaches to solving the inverse problem, use of a more realistic head model will lead to more accurate localization results.

Finally, we demonstrated in Section V-B that the choice of reference does not impact the accuracy of the solution provided the $\mathbf{H}(\mathbf{q})$ is determined with respect to the chosen reference. In clinical EEG, the reference choice often plays an important role in distinguishing relevant activity from background signals. Our method may resolve some of these issues since it appears to generate reference independent solutions. We note that our method may also be applied to the so-called bipolar montage that is often used to distinguish locally generated signals from noise. This montage does not employ a common reference, but rather each electrode is referenced to its neighbor; in effect, a spatial derivative is computed. The spatial filtering approach can be applied to such data by determining $\mathbf{H}(\mathbf{q})$ in a bipolar fashion. That is, the columns of $\mathbf{H}(\mathbf{q})$ represents the differences between neighboring electrodes associated with a unit dipoles oriented in the x, y, and z coordinate directions at location $\mathbf{q}$.

The results presented in this paper suggest that the spatial filtering approach has considerable potential as a source localization tool. The method gives good results under realistic conditions and is robust to deviations in the assumed signal model. Additional experience with real data is needed to fully validate the effectiveness of this technique.

REFERENCES

[1] D. H. Fender, "Source localization of brain electrical activity," in *Methods of Analysis of Brain Electrical and Magnetic Signals. EEG Handbook*, revised series, A. S. Gevins and A. Remonds, Eds. Amsterdam: Elsevier, 1987, vol. 1, pp. 355–403.

[2] R. N. Kavanagh, T. M. Darcey, D. Lehman, and D. H. Fender, "Evaluation of methods for three-dimensional localization of electrical sources in the human brain," *IEEE Trans. Biomed. Eng.*, vol. BME-24, pp. 421–429, 1987.
[3] J. W. H. Meijs, "The influence of head geometries on electro- and magnetoencephalograms," Ph.D. thesis, Enschede, Netherlands, 1988.
[4] P. L. Nunez, "Methods to estimate spatial properties of dynamic cortical source activity," in *Functional Brain Imaging*, G. Pfurtscheller and F. Lopes da Silva, Eds. Toronto: Hans Huber, 1988, pp. 3–10.
[5] J. C. de Munck, "A mathematical and physical interpretation of the electromagnetic field of the brain," Ph.D. thesis, University of Amsterdam, Amsterdam, the Netherlands, 1989.
[6] Y. Salu, L. G. Cohen, D. Rose, S. Sato, C. Kufta, and M. Hallett, "An improved method for localizing electric brain dipoles," *IEEE Trans. Biomed. Eng.*, vol. 37, pp. 699–705, 1990.
[7] M. Scherg, "Fundamentals of dipole source potential analysis," in *Auditory Evoked Magnetic Fields and Electric Potentials. Advances in Audiology*, F. Grandori, M. Hoke, and G. L. Romani, Eds. Basel, Switzerland: Karger, 1990, vol. 6, pp. 40–69.
[8] M. Scherg, "Functional imaging and localization of electromagnetic brain activity," *Brain Topogr.*, vol. 5, pp. 103–111, 1992.
[9] Y. Yan, P. L. Nunez, and R. T. Hart, "Finite-element model of the human head: Scalp potentials due to dipole sources," *Med., Biol. Eng. Comput.*, vol. 29, pp. 475–481, 1991.
[10] J. C. Mosher, P. S. Lewis, and R. M. Leahy, "Multiple dipole modeling and localization of spatio-temporal MEG data," *IEEE Trans. Biomed. Eng.*, vol. 39, pp. 541–557, 1992.
[11] B. Van Veen, J. Joseph, and K. Hecox, "Localization of intra-cerebral sources of electrical activity via linearly constrained minimum variance spatial filtering," in *Proc. IEEE Workshop on Statistical Signal and Array Processing*, Oct. 1992, pp. 526–529.
[12] A. M. Dale and M. I. Sereno, "Improved localization of cortical activity by combining EEG and MEG with MRI cortical surface reconstruction: A linear approach," *J. Cognitive Neurosci.*, vol. 5, no. 2, pp. 162–176, 1993.
[13] B. J. Roth, M. Balish, A. Gorbach, and S. Sato, "How well does a three-sphere model predict positions of dipoles in a realistically shaped head?" *Electroenceph. Clin. Neurophysiol.*, vol. 87, pp. 175–184, 1993.
[14] A. Amir, "Uniqueness of the generators of brain evoked potential maps," *IEEE Trans. Biomed. Eng.*, vol. 41, pp. 1–11, 1994.
[15] Z. Zhang and D. L. Jewet, "DSL and MUSIC under model misspecification and noise-conditions," *Brain Topogr.*, vol. 7, pp. 151–161, 1994.
[16] T. C. Liu and B. Van Veen, "Multiple window based minimum variance spectrum estimation for multidimensional random fields," *IEEE Trans. Signal Processing*, vol. 40, pp. 578–589, Mar. 1992.
[17] B. Van Veen and K. Buckley, "Beamforming: A versatile approach to spatial filtering," *IEEE ASSP Mag.*, vol. 5, pp. 4–24, Apr. 1988.
[18] R. T. Lacoss, "Adaptive combining of wideband array data for optimal reception," *IEEE Trans. Geosci. Electron.*, vol. GE-6, pp. 78–86, May 1968.
[19] O. L. Frost, "An algorithm for linearly constrained adaptive array processing," *Proc. IEEE*, vol. 60, pp. 926–935, Aug. 1972.
[20] B. Van Veen, J. Joseph, and K. Hecox, "Method and apparatus for localization of intracerebral sources of electrical activity," US Patent 5 263 488, Nov. 23, 1993.
[21] M. E. Spencer, R. M. Leahy, J. C. Mosher, and P. S. Lewis, "Adaptive filters for monitoring localized brain activity from surface potential time series," in *Conf. Rec. 26th Annu. Asilomar Conference on Signals, Systems, and Computers*, Nov. 1992, pp. 156–161.
[22] W. van Drongelen, M. Yuchtman, B. Van Veen, and A. van Huffelen, "Spatial filtering applied in source localization of electrical activity in the brain," *Brain Topogr.*, vol. 9, pp. 39–49, 1996.
[23] B. Widrow, K. M. Duvall, P. P. Gooch, and W. C. Newman, "Signal cancellation phenomena in adaptive arrays: Causes and cures," *IEEE Trans. Antennas Propagat.*, vol. AP-30, pp. 469–478, May 1982.
[24] J. Capon and N. R. Goodman, "Probability distributions for estimators of the frequency-wavenumber spectrum," *Proc. IEEE*, vol. 58, pp. 1785–1786, Oct. 1970.
[25] M. S. Buchsbaum, E. Hazlett, N. Sicotte, R. Ball, and S. Johnson, "Geometric and scaling issues in topographic electroencephalography," in *Topographic Mapping of Brain Electrical Activity*, F. H. Duffy, Ed. Boston, MA: Butterworths, 1986, pp. 325–337.
[26] J. C. de Munck, "The estimation of time varying dipoles on the basis of evoked potentials," *Electroenceph. Clin. Neurophysiol.*, vol. 77, pp. 156–160, 1990.
[27] M. Scherg, "From EEG source localization to source imaging," *Acta Neurol. Scand., Supplement*, vol. 152, pp. 29–30, 1994.

Barry D. Van Veen (S'81–M'86) was born in Green Bay, WI. He received the B.S. degree from Michigan Technological University, Houghton, in 1983 and the Ph.D. degree from the University of Colorado, Fort Collins, in 1986, both in electrical engineering. He was an ONR Fellow while working on the Ph.D. degree.

In the spring of 1987, he was with the Department of Electrical and Computer Engineering at the University of Colorado–Boulder. Since August of 1987, he has been with the Department of Electrical and Computer Engineering at the University of Wisconsin–Madison and is currently a Professor. His research interests include signal processing for sensor arrays, nonlinear systems, adaptive filtering, acoustical, and biomedical applications of signal processing.

Dr. Van Veen was a recipient of the 1989 Presidential Young Investigator Award and the 1990 IEEE Signal Processing Society Paper Award. He is currently an Associate Editor for the IEEE TRANSACTIONS ON SIGNAL PROCESSING and served on the IEEE Signal Processing Society's Technical Committee on Statistical Signal and Array Processing from 1991 through 1997.

Wim van Drongelen was born in Vlissingen, The Netherlands, in 1953. He studied biophysics at Leiden University, Leiden, Netherlands. After a period in the Laboratoire d'Electrophysiologie, Universite Claude Bernard, Lyon, France, he received the M.S. degree. In 1980, he received the Ph.D. degree.

From 1977, he worked for The Netherlands Organization for the Advancement of Pure Research (ZWO) in the Department of Animal Physiology, Wageningen, Netherlands. He worked for the HBO Institute Twente, Netherlands. He taught neurophysiology and neuroanatomy and founded a Medical Technology Department. In 1986, he started to work for Nicolet Instrument, the Netherlands, as a Benelux Application Engineer. From 1990 to 1993, he was international Application Specialist and he managed the Dutch office of Nicolet Instrument. In 1993, he relocated to Madison, WI. He is Senior Application Engineer with the Engineering Department of Nicolet Biomedical, Inc. His ongoing research interests are in source localization, pattern recognition algorithms, and application of electrophysiology in monitoring.

Moshe Yuchtman was born in Tel Aviv, Israel, in 1948. He received the B.Sc. degree from Tel Aviv University in 1972. He received his M.Sc. degree in neurobiology from the Hebrew University in Jerusalem, Israel, in 1976. In 1982, he received the M.Sc. degree in speech and hearing science from the University of Illinois, Urbana-Champaign. He worked as a Research Associate with the Speech Research Laboratory of the University of Indiana, Bloomington, between 1984 and 1987.

Since 1987, he has been with Nicolet Biomedical as an Application Research Engineer. He has been involved in the development of applications of signal processing in neurophysiology and speech perception.

Akifumi Suzuki was born in Ooshima, Tokyo, Japan, in 1949. He received the M.D. degree from the Prefectural University of Mie in 1974. He specialized in surgery and neurosurgery with the Matsuka Central Hospital and the Research Institute for Brain and Blood Vessels, Akita, Japan. In 1980, he was a board qualified neurosurgeon. He received the D.MSc. degree from the Tohoku University, Japan, in 1982.

Currently, he has several functions with the Research Institute for Brain and Bloodvessels, Akita, Japan. He is Director of the Department of Cerebral Apoplexy, Chief of Neurosurgery, Chief Researcher of Surgical Neurology, and Chief of the Intensive Care Unit. He is author of more than 100 scientific articles.

Dr. Suzuki has received several awards for his work. Among them are: special symposist in the 50th Memorial Congress of the Japan Neurosurgical Society and the Nakamura Memorial Prize, and fellowship in the American College of Angiology.